(This is a sample cover image for this issue. The actual cover is not yet available at this time.)

Computers & Fluids 71 (2013) 196–207

Contents lists available at SciVerse ScienceDirect

Computers & Fluids

journal homepage: www.elsevier.com/locate/compfluid

A population balance-Monte Carlo method for particle coagulation in spatially inhomogeneous systems

Haibo Zhao *, Chuguang Zheng

State Key Laboratory of Coal Combustion, Huazhong University of Science and Technology, Wuhan, PR China

ARTICLE INFO

Article history:
Received 23 November 2010
Received in revised form 11 July 2012
Accepted 23 September 2012
Available online 6 November 2012

Keywords:
Population balance
Monte Carlo
Multiphase flow
Coagulation
Four-way coupling

ABSTRACT

Insight into the spatiotemporal evolution of particle size distribution (PSD) is very useful in many natural and engineering systems in which the multiphase fields are spatially inhomogeneous and complicated dynamic processes of particle population, e.g., coagulation between particles, occur with field-dependent rates. Traditional population balance modeling (PBM) is usually used to simulate spatially homogeneous dynamic processes, only obtaining the time evolution of PSD. In this paper, we presented an algorithm to predict the spatiotemporal evolution of PSD accounting for mutual coupling of particle population and hydrodynamics. The differentially-weighted Monte Carlo method for PBM is used to simulate coagulation behavior of particles in each grid that is considered to be spatially homogeneous, and the transport behavior of fluid and particles towards neighbor grids that are spatially inhomogeneous are described by general conservation equations of multiphase flows. The simulation strategy is based on the selection of a time step within which the fluid transport, the particle transport and the particle dynamics are uncoupled and then separately simulated. A limiting case of the coarse high-inertia particles whose motion is independent of surrounding fluid is chosen to validate the population balance-Monte Carlo (PBMC) method for the spatiotemporal evolution of PSD. The computational time is found to be less by a factor of 10 compared to the direct numerical simulation (DNS), yielding reasonably closer predictions of spatiotemporal particle size distributions.

1. Introduction

Population balance modeling (PBM) has been a state of great interest for industrial applications such as crystallization, precipitation, combustion, aerosol, milling, pharmacy, and granulation. Great efforts have been made to further develop the methodology [1,2]. Traditional PBM usually simulates presumed spatially homogeneous dispersed systems and only captures the temporal evolution of particle size distribution (PSD). In fact, if only volume averaged (spatially-averaged) population balance equation (PBE) is used as the macro-continuity equation to characterize the complex particle–fluid systems, it is the zero-dimensional simulation. The zero-dimensional PBM may explore some basic characteristics of dispersed systems to a certain extent, however, fails to obtain the detailed information on spatially-resolved multiphase flow fields and dynamic evolution. Furthermore, in the zero-dimensional PBM the interaction between continuous and discrete phases is neglected. In order to achieve accurate control of particulate processes, optimized design and operation of corresponding process equipments, the numerical analysis of temporally and spatially inhomogeneous PSD should be considered [3], as almost every industrial processes will have spatial inhomogeneities. Furthermore, the occurrence rates (characterized by "kernels") of dynamic events involved in particle population are generally dominated by, or, at least, dependent of their surrounding multiphase fluid fields. As a example, the turbulent transport effect and the preferential concentration effect lead to an increase of inter-particle collision rates by a factor of as much as 30 [4]. Thus, for an accurate modeling the particle dynamics and hydrodynamics have to be solved simultaneously to obtain the spatiotemporal evolution of particle population in spatially inhomogeneous systems. In this sense, the PBM for particle dynamics has to couple with multiphase flow models for hydrodynamics.

The mutual coupling of the PBM with the multiphase flow models faces enormous challenges based on issues of formulation as well as computation [1]. For example, most multiphase flow models are not capable of treating widely-distributed polydispersed particle population that is a typical characteristic during dynamic evolution of particles even through their distribution is monodisperse in the initial stage. Moreover, it is difficult to consider the exchange and transport of momentum, mass and energy between the continuous and discrete phases as well as between the discrete phases (i.e., the effect of four-ways coupling). As far as only pairwise coagulation event and only one internal state of particles, particle size, are considered here, the mathematical formulation

* Corresponding author. Tel.: +86 27 8754 4779; fax: +86 27 8754 5526.
E-mail address: klinsmannzhb@163.com (H. Zhao).

0045-7930/$ - see front matter © 2012 Elsevier Ltd. All rights reserved.
http://dx.doi.org/10.1016/j.compfluid.2012.09.025

of the change in the continuous particle size distribution function (PSDF) with time and position is given by generalizing the equation of convective diffusion into the Smoluchowski equation [5]:

$$\frac{\partial n}{\partial t}+\nabla\cdot n\mathbf{u}=\nabla\cdot D\nabla n-\nabla\cdot\mathbf{c}n+\frac{1}{2}\int_0^{v_p}\beta(\tilde{v}_p,v_p-\tilde{v}_p)n(\tilde{v}_p)n(v_p-\tilde{v}_p)d\tilde{v}_p-\int_0^{\infty}\beta(v_p,\tilde{v}_p)n(v_p)n(\tilde{v}_p)d\tilde{v}_p \quad (1)$$

where n is the particle size distribution function; D is the coefficient of diffusion; $\mathbf{c}$ is the particle migration velocity resulting from the external force field; $\mathbf{u}$ is the fluid velocity; $\beta(v_p,\tilde{v}_p)$ is the coagulation kernel for two particles of volume v_p and $\tilde{v}_p$, $m^3\,s^{-1}$. The third term on the right-hand of Eq. (1) is the birth term of coagulation processes, accounting for the formation of a particle of volume v_p due to the coagulation event between a particle of volume $\tilde{v}_p$ (smaller than v_p) and a particle of volume $(v_p-\tilde{v}_p)$; and the coefficient 1/2 is raised from the fact that one coagulation event is related to two particles. The forth term is the death term, representing the disappearance of a particle of volume $\tilde{v}_p$ due to coagulation event with any other particle.

As a first step of the coupling between the PBM and the multiphase flow models, in many studies for the particulate processes (as examples, see Refs. [6–9]) a one-way coupling is assumed, i.e., the particulate particle phase is assumed to have negligible influence on the surrounding fluids so that the continuous phase can be simulated by general Eulerian models even commercial CFD (computational fluid dynamics) solvers independently. Using the spatially inhomogeneous flow fields obtained in advance and assuming that the transport of particles occurs solely by convection and diffusion, particle dynamics in each grid that is considered to be spatially homogeneous is captured by the PBM and the spatiotemporal evolution of PSD is thus obtained [10–12]. The one-way-coupling CFD–PBM simulation is easy to realize numerically and program. Studies on coupling of the PBM with the Eulerian models or CFD calculations can be classified according to the numerical methods applied for PBM, which could be monodisperse methods [13], moments methods [14–23], sectional methods [24–30], Monte Carlo methods [31–37], or other novel methods [38–43]. With regards to the one-way-coupling simulation strategy, the conservation equations of the discrete phase are not solved simultaneously and the interaction between the continuous phase and entrained discrete particles are left out of account. It is feasible for simulating the particulate processes and micro-scale particles because the particle displacement relative to the fluid element path and the influence of the particle phase on the fluid phase are negligible. From the viewpoint of multiphase flow simulation, the one-way coupling is reasonable when the fractional volume Φ_v and mass loading Φ_m of particles are small (e.g., $\Phi_v<10^{-4}$). However, when Φ_v increases or when the phenomenon of preferential accumulation results in obvious nonuniform distribution of particles, the effect of the turbulent carrier flow on the dynamics of the dispersed phase and the back influence of the dispersed phase on the carrier-phase dynamics should be considered simultaneously (i.e., the two-way and even four-way coupling between the two phases). In many of multiphase processes the coupling between the continuous and discrete phases can become significant due to mass, momentum and energy transfer, and neglecting such two-ways-coupling effects may lead to erroneous prediction and understanding of overall system behavior [44]. It is thus necessary to couple particle dynamics (using the PBM) and not only fluid behavior but also transport and motion of particles (using the multiphase flow models) in these circumstances. Unfortunately, attempts to incorporate the PBM into multiphase flow models have been limited.

As known, the multiphase flow models can fall into two categories according to the simulation methodology of the discrete phases in an Eulerian reference frame or in a Lagrangian reference frame, saying, the two-fluids models (Eulerian–Eulerian models) or the fluid-trajectory models (Eulerian–Lagrangian models). Similarly, the numerical methods of PBM can be divided into deterministic and stochastic. On the deterministic front, the differential equations depicting the population balance, population balance equations (PBEs), are directly solved through integration using appropriate techniques, e.g., an discretization scheme towards particle size distribution (as in (discrete)-sectional methods) and a presumed monodisperse or log-normal PSD (as in moments methods). In contrast to deterministic integration, stochastic methods utilize Monte Carlo (MC) to simulate the evolution of a finite sample of the particle population. Obviously, the deterministic methods for PBM, which are based on the Eulerian reference frame and the PBE can be solved by ODE (ordinary differential equation) solvers together with the conservation equations of multiphase flows, are capable of coupling into the Eulerian–Eulerian models for hydrodynamics. As an example, Yeoh and Tu [45] presented a two-fluid model coupled with population balance approach to predict sub-cooled boiling flow at low pressure in a vertical annular channel, which is implemented in the computer code CFX4.4. However, the Eulerian–Eulerian model and the deterministic PBM method, which are based on the calculation scheme of volume/ensemble/mass-weighted averaging, exhibit relatively lower resolution on the particle dynamics. In fact, the Eulerian–Eulerian model is restricted within monodisperse particles (usually, the polydisperse particles are viewed as monodisperse particles in the model), and is thus unable to consider the polydispersity effect and cross-scale effect of particles (in fact, these effects are typical characteristics in the particle dynamics). Furthermore, the deterministic PBM method cannot gain information about history, trajectory crossing and internal structure of particles. The deterministic PBM method is also less sensitive to the innate fluctuations for dynamic processes which are also stochastic in nature. Besides these, the deterministic PBM methods are generally formulated by complicated mathematical equations, and are at the disadvantage of the modeling of more than two particle properties (such as size, chemical composition, surface area, and charge level). On the other hand, the stochastic methods for PBM (such as Monte Carlo techniques) are able to simulate any number of particle properties and are easily programmed. Although the population balance-Monte Carlo (PBMC) methods exhibit relatively higher computational expense due to the large number of simulation particles that need to be tracked in order to provide a statistically reasonable representation of the physics, the high-speed development of computer hardware (CPU and memory) and parallel computing motivates their practical applications. As the PBMC methods are methodically closer to the Lagrangian approach, they are more suitable for coupling into the Eulerian–Lagrangian models to obtain the spatiotemporal evolution of particle population. Until now, however, the coupling of the PBMC methods and the Eulerian–Lagrangian models has not been reported.

Since the PBMC methods generally require expensive computational cost and exhibit statistical noise, it is very important for the PBMC methods to utilize limited number of simulation particles to reach an acceptable accuracy. In recent years several PBMC methods have been developed to keep the total number of simulation particles within prescribed bounds, even though the number concentration of real particles changes dramatically. Prominent among these are the constant-number method by Matsoukas et al. [46,47] and the differentially weighted MC method by us [48,49] and other scientists [50,51]. Through filling continuously the empty sites due to, e.g., coagulation event, with copies of the surviving particles, or discarding continuously some surviving particles to insert some

new particle from, e.g., breakage event, the total number of simulation particles is maintained in the constant-number method. At the same time, the waiting time between two successive events adjusts itself to the rates of the corresponding dynamic processes. The constant-number method uses equally-weighted simulation particles in nature. With regard to the differentially-weighted MC method, the simulation particles have different private weights. The event probability of one simulation particle relates to not only its rate of corresponding dynamic process but also its private weight. The total number of simulation particles is kept constant by adjusting their private weights to the corresponding dynamic events. We will briefly introduce this method in Section 2. Although constant number of simulation particles is very useful to guard statistical accuracy, it must be noted that the PBMC methods may still perform a great deal of statistical noise for particle size distribution function if there is an insufficient number of simulation particles in some areas of size spectrum. For example [49], even when millions of simulation particles are used in the PBMC methods, there may still be only several simulation particles or even no simulation particle at the edges of a lognormal size distribution if simulation particles are equally weighted. In order to determine accurately the particle size distribution over the full size range, not only the total number of simulation particles but also the simulation particle number in each section of size spectrum should be guaranteed within appropriate bounds. In other words, it is necessary to specify a finite number of simulation particles to distribute over size spectrum homogeneously. It is not possible with the constant-number method to restrict the simulation particle number in each section of size spectrum within prescribed bounds due to its inherent equally-weighting scheme. On the contrary, in the differentially-weighted MC method [48,49], sufficient simulation particles can be placed in these less-populated areas of the size spectrum and the simulation particle number in densely-populated areas can be limited by consideration and recalculation of individual weights, which makes the differentially-weighted MC method protect against its statistical noise in the calculation of PSD and constrain at the same time its computational expense. We also noticed that the stochastic weighted particle method [50] recently proposed by Patterson, Wagner and Kraft and the weighted flow algorithm [51] recently proposed by DeVille, Riemer, and West exhibit good performance as our differentially-weighted MC.

In this paper, we present a simulation strategy to couple the differentially-weighted MC method for particle dynamics with the general Eulerian–Lagrangian models for hydrodynamics. The simulation strategy is based on the selection of a time step within which the fluid transport, the particle transport and the particle dynamics are uncoupled and then separately simulated. The resultant Eulerian–Lagrangian–PBMC model (or call it the CFD–PBM model) is able to account for the fluid–particle interaction and the particle dynamics (the particle–particle interaction in a sense) in theory. Among the various particle dynamic mechanisms, particle coagulation is the most demanding mechanisms for modeling, as it always involves interaction between different particles. This paper aims to the spatiotemporal evolution of PSD due to particle coagulation and the transport of their surrounding multiphase fluids. A limiting case of the coarse high-inertia particles in which analytical coagulation kernel exists is used to validate the model by comparing it with direct numerical simulation (DNS, as a benchmark).

2. Model description

2.1. The simulation strategy of coupling the PBMC method for particle dynamics with the Eulerian–Lagrangian model for hydrodynamics

The Eulerian–Lagrangian model is one of the most popular models simulating the two-phase flow fields. The transport of the continuous phase in the Eulerian reference frame is based on its conservation equations of mass, momentum and energy, which can be formulated by the following general representation:

$$\frac{\partial(\rho\phi)}{\partial t}+\frac{\partial(\rho u_j\phi)}{\partial x_j}=\frac{\partial}{\partial x_j}\left(\Gamma_\phi\frac{\partial\phi}{\partial x_j}\right)+S_\phi \tag{2}$$

where ϕ is a general transport variable which could be 1 (for the continuity equation), u_j (fluid velocity, for the momentum equation) and h (enthalpy, for the energy equation); ρ is fluid density; Γ_ϕ is diffusion coefficient dependent of ϕ; S_φ is ϕ-dependent source term which should consider the effect of the discrete phase on the continuous phase. There are numerous studies on S_ϕ and the closure of the conservation equations, and many models, for example, Reynolds stress model [52], appear in open references.

In a Lagrangian reference frame, the transport equations on the position and velocity of a particle can be written as [53]:

$$\frac{dx_{\mathrm{p}i}}{dt}=u_{\mathrm{p}i} \tag{3}$$

$$\frac{du_{\mathrm{p}i}}{dt}=g_i+\frac{1}{\tau_{\mathrm{p}}}(u_i-u_{\mathrm{p}i})+F_{\mathrm{other}} \tag{4}$$

where $x_{\mathrm{p}i}$ and $u_{\mathrm{p}i}$ are the position and velocity of a particle; g_i is the gravitational acceleration; τ_{p} is the particle relaxation time for particle motion due to the effect of the viscous drag force; and F_{other} is other force terms contributing to particle transport.

The paper pays particular attention on the coupling strategy of the PBM and the multiphase flow model, and the detailed models for multiphase flows are thus not discussed here. Since the multiphase flow simulators work with standard integrators that are time-driven, it is possible to integrate the PBMC method and the Eulerian–Lagrangian model into a same framework. The classical direct simulation Monte Carlo (DSMC) for gas dynamics (firstly proposed by Bird [54]) used a small time step to insure the movement of gas molecules can be decoupled from the collision processes of gas molecules. Illumined by the idea, the coupling strategy adopted here is based on the appropriate selection of time-step within which the coupling between particle behavior and fluid flow is neglected. Within an appropriate time-step, it is considered that not only the flow transport and the particle transport are uncoupled each other, but also the particle transport and the particle dynamics are uncoupled each other. So the flow fields characterized by Eq. (2), the particle fields by Eqs. (3) and (4) and the particle size distribution by the PBE are independently solved within the time-step. As mentioned above, the kernels of dynamic events, e.g., the coagulation kernel $\beta_{ij}(x_k,t)$, which models the occurrence probability of coagulation event between any two particles i and j at time t and space position x_k, is usually dependent of environmental variables of two-phase flows. Thus, within a time-step two-phase flow fields should be firstly simulated using the Eulerian–Lagrangian models, without consideration of particle dynamics. Using the two-phase flow fields, spatiotemporally-dependent coagulation kernels can be calculated. Then the PBMC method is used to capture particle coagulation events in each grid. Coagulation dynamics results in changes of particle fields. Based on these new particle fields, the two-phase flow fields within next time step are calculated. By the exchange of the environmental variables of the continuous and discrete phases within the time-step, the fluid–particle interaction as well as the particle–particle interaction is considered at the same time. We plot Fig. 1 to demonstrate the coupling of the population balance and the hydrodynamics. Obviously the key points are to select an appropriate time-step to ensure the uncoupling of flow transport, particle transport and particle coagulation, and, to simulate spatiotemporally-dependent coagulation process, which will introduced in

the following text. The resultant Eulerian–Lagrangian–PBMC model (its flowchart is shown in Fig. 2) can be numerically solved through the following steps.

Step 1: the boundary conditions are characterized, and the space grids are plotted; the fields of two-phase flows are initialized, and the simulation particles with prescribed number are generated to represent these real particles;
Step 2: Monte Carlo loop starts with different seeds for the random number generator. Several MC loops (in general, 3–5 loops) are performed to obtain adequate statistical data. The average quantities are used as output of the numerical simulation;
Step 3: Time-step loop starts according to the procedure of time-driven technique, i.e., the time window $[t_{start}, t_{end}]$ is discretized into a number of time-steps by some laws, which will be described in Section 2.2.
Within one time-step, Steps 4–9 are performed in turn;
Step 4: the nth time-step, Δt_n, is estimated according to the two-phase flow fields as well as the particulate processes at the end of Δt_{n-1}. The appropriate time-step ensures the uncoupling of flow motion, particle motion and particle dynamics;
Step 5: the conservation equations of the continuous phase, i.e., Eq. (2), are numerically solved by, for example, an extended version of SIMPLE-C (Semi-Implicit Method for the Press-Linked Equation-Consistent) algorithm. The flow field profiles (i.e., the mean velocity $\bar{u}_i$, the stress $\bar{p}$, the Reynolds stresses $\overline{u_{gi}u_{gj}}$, the turbulent kinetic energy k, the dissipation rate of turbulent kinetic energy ε, etc.) are obtained. The interaction source term is calculated according to the instantaneous behavior of marking particles in the local grid.
Step 6: the motion of each simulation particle is tracked in parallel. The particle spatial position (x_{pi}) and the particle velocity (u_{pi}) evolve following Eqs. (3)-(4), which can be solved by, e.g., a second-order Runge–Kutta method.
Step 7: the dynamic evolution of particle population is handled. Any possible dynamic events of simulation particles in a grid are described within Δt_n. The detailed schemes will be introduced in Section 2.3;
Step 8: the environmental variables of the discrete phase including the particle number density ($\bar{N}_p$), the averaged particle velocities ($\bar{u}_{pi}$) and the particle Reynolds stress ($\overline{u_{pi}u_{pj}}$), are determined by the ensemble averaging procedure over all simulation particles in their local grid; these statistical parameters will be used by the Eulerian–Lagrangian–PBMC model for multiphase flow fields during the next time iteration. Simultaneously, the particle source term is obtained by the scheme of particle-source-in-cell (PSIC) [55], and then is added to the flow-phase conservation equations at the beginning of the next time iteration. The two-phase interaction is considered by the exchange of flow fields and particle fields;
Step 9: the simulator returns to Step 3 if $\Sigma_n \Delta t_n < t_{end}$; otherwise, the current time loop is finished and the next MC loop is started;
Step 10: if the number of MC loops is less than the specified value, the simulator returns to Step 2 and the new MC loop is started; otherwise, the simulator moves to the next step;
Step 11: the averaging on the several MC loops is taken, and the averaged parameters of two-phase flow fields are outputted.

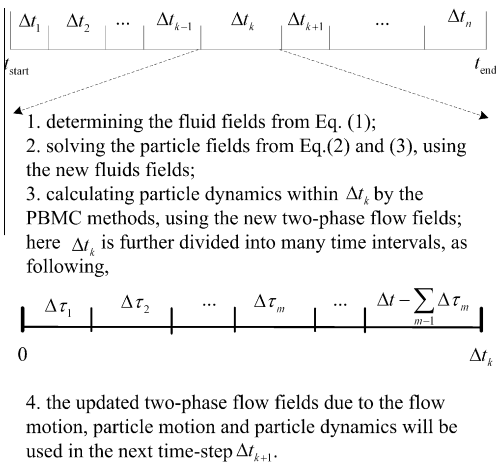

Fig. 1. The coupling strategy of population balance modeling (PBM) and multiphase flow models.

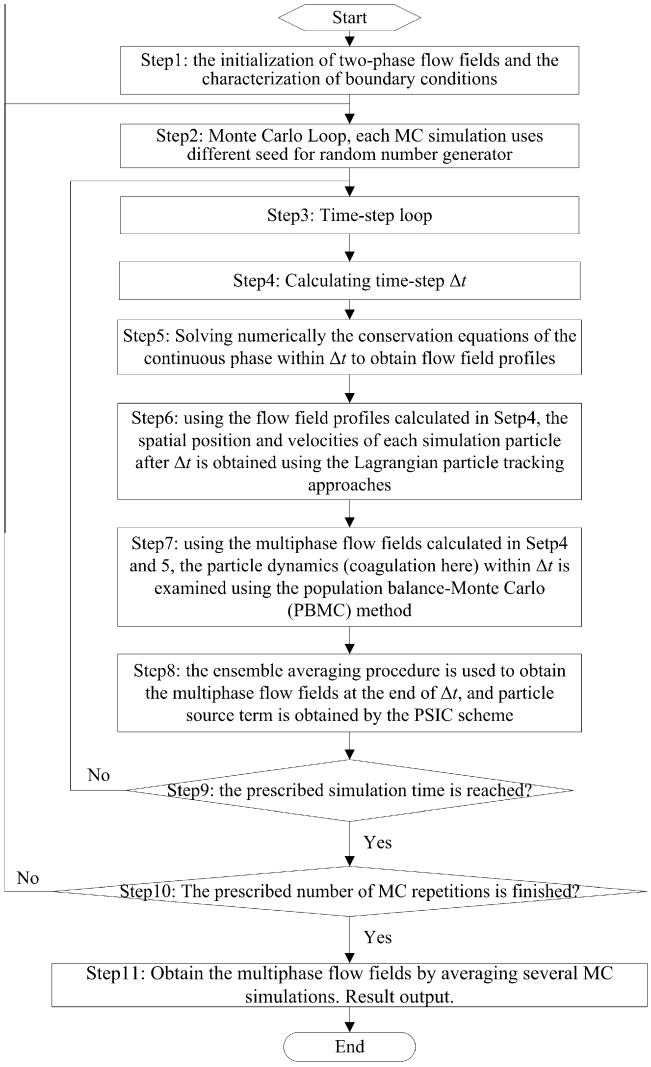

Fig. 2. The flowchart for the Eulerian–Lagrangian–PBMC model.

2.2. The determination of time-step

In order to achieve the uncoupling of the flow motion and the particle motion, the time-step should be less than the particle relaxation time scale τ_p and the eddy lifetime T_e (or, the fluid integral time scale seen by the particle. T_e can be estimated from the local turbulence properties, $T_e = k/(\alpha\varepsilon)$, where α is a model

parameter (for example, in the eddy interaction model Gosman and Ionnides [56] take α as constant number of 4.978)) [57]. On the other hand, other special requirements for the time-step are set in order to take into account particle dynamics by the PBMC method.

In the first place, time-step is constrained to be less than the crossing time scale of fluid element to the grid:

$$\Delta t \leq \min\{L_{l,k}/|u_{pk,i}|\} \tag{5}$$

where $L_{l,k}(k = 1, 2, 3)$ is the length of the grid l in different directions, and $u_{pk,i}$ is the k-direction velocity of particle i. By Eq. (5), the particle moves in the same grid or to the neighboring grids within Δt. In addition, it is usually assumed that a simulation particle i located in grid l may only coagulate with another particle located in the same grid l. As a result, the computational cost of checking the particle coagulation events using the PBMC method will be sharply cut down because the double circle over all grids and all particles is avoided.

In order to realize the uncoupling of dynamic events, particle i is restricted to participate in at most one coagulation event within a time step (although it is possible the total number of coagulation events within the grid l and the time step is far greater than 1), that is,

$$\Delta t \leqslant t_{i,\mathrm{coag}} = 1/(V_{cl}C_{i,l}) \tag{6}$$

where $t_{i,\mathrm{coag}}$ is the time interval of two successive coagulation events of particle i; V_{cl} is the volume of grid l; $C_{i,l}$ (with dimension of $s^{-1}\,m^{-3}$) is the total coagulation probability of particle i. In our differentially-weighted MC method, a new probabilistic coagulation rule for coagulation events between two differentially weighted simulation particles is derived [48]. In this rule, for a coagulation event between simulation particle i and j, it is imagined that each real particle from i undergoes a real coagulation event with a probability of $\min(w_i, w_j)/w_i$, and each real particle from j does so with a probability of $\min(w_i, w_j)/w_j$, where w_i and w_j are the private weights of particles i and j, respectively. On the basis of the rule, $C_{i,l}$ is calculated as:

$$C_{i,l} = \frac{1}{V_{cl}^2}\sum_{j=1,i\neq j}^{N_{st,l}}\left[\frac{2\beta_{ij}(l,t)w_j\max(w_i,w_j)}{w_i+w_j}\right] = \frac{1}{V_{cl}^2}\sum_{j=1,i\neq j}^{N_{st,l}}[\beta'_{ij}(l,t)] \tag{7}$$

where $N_{st,l}$ is the total number of simulation particles in the grid l; $\beta'_{ij}(l,t)$ is a normalized kernel in the differentially-weighted MC method that relates not only to the particle states (particle size, position, velocity and other flow field parameters) but also to their weights of the two simulation particles.

To sum up, the time-step is restricted to implement the uncoupling between the flow motion, the particle motion and the particle dynamics, as follows:

$$\Delta t \leqslant \min\left\{\tau_p, T_e, \min_{\forall l,\forall i,\forall k}\left\{L_{l,k}/u_{pi,k}\right\}, \min_{\forall l,\forall i}\{1/(V_{cl}C_{i,l})\}\right\} \tag{8}$$

Using the time step determined by Eq. (8), it is concluded that the evolution of systems is based on the process (the flow and particle transport, or particle dynamics) that occurs most rapidly. If particulate events such as coagulation are slow, the multiphase flow fields update due to their flow, resulting in the spatial diffusion of PSD. If on the other hand, the dynamic events of particles are fast relative to particle transport, the particle fields evolve due to their transport and dynamics, resulting in the spatiotemporal evolution of PSD.

2.3. The simulation of coagulation event within a grid and an adjustable time-step

The MC simulation of the population balance bases on converting kinetic rate equations into probabilities and selecting the relevant events by means of random numbers. It differs notably from the Lagrangian particle tracking method in that no information about the particle spatial position is needed. Although the exact position of simulation particle can be obtained using the Eulerian–Lagrangian model described above, in the PBMC method the simulation particles have no exact position but belong to a grid. In a grid the multiphase flow fields are considered to be spatially homogeneous, while spatially inhomogeneous among different grids. Thus, the general PBMC method for particle dynamics in a presumed spatially homogeneous system can be directly used to capture coagulation dynamics within a prescribed time step Δt (by Eq. (8)) and within each grid in parallel. Here the differentially-weighted MC method is introduced.

As a first step, at the end of time-step Δt the total coagulation probability of a particle i in a grid l is recalculated using the new multiphase flow fields that are different from the fields at the beginning of Δt due to flow motion and particle motion within Δt.

Then, the time interval for coagulation dynamics is considered to be less than the waiting time between two successive coagulation events for a simulation particle, i.e.,

$$\Delta\tau = pN_{st,l}\Big/\sum_{i=1}^{N_{st,l}}(V_{cl}C_{i,l}) \tag{9}$$

where p is a specified experience parameter, representing the ratio of the coagulated simulation particle number within grid l and $\Delta\tau$ to $N_{st,l}$. p has a value between $2/N_{st,l}$ and 1, and is usually set around 0.01–0.05.

Within the third step, a jump Markov model for particle coagulation is constructed, that is, within the time interval $\Delta\tau$ the interacting particle pairs are selected with probability $\beta'_{ij}/\sum_i\sum_{j,j\neq i}\beta'_{ij}$. Each simulation particle within grid l is examined successively to determine whether the particle coagulates within $\Delta\tau$ and V_{cl}, and, if the particle coagulates, who is its partner. As for simulation particle i, the probability of a coagulation event of i taking place within $\Delta\tau$ and V_{cl} is an exponentially distributed random variable, that is:

$$P'_{\mathrm{coag},i}(\Delta\tau) = 1 - \exp(-V_{cl}C_{i,l}\Delta\tau/2) \tag{10}$$

Once a random number r from a uniform distribution in the interval [0,1] is less than $P'_{\mathrm{coag},i}(\Delta\tau)$, i is allowed to coagulate. The coagulation partner of particle i is then found based on the probability $P'_{ij}\left(=\beta'_{ij}/\sum_{k=1,k\neq i}^{N_{st}}\beta'_{ik}\right)$. Usually, either the cumulative probabilities method or the acceptance–rejection method is used to select the coagulation partner. In the cumulative probabilities method, simulation particle j is the coagulation partner once the following condition is met:

$$\sum_{k=1}^{j-1}P'_{ik} \leqslant r \leqslant \sum_{k=1}^{j}P'_{ik} \tag{11}$$

While in the acceptance–rejection method, a randomly selected particle j is accepted as coagulation partner of i if the following condition is met:

$$r \leq \beta'_{ij}/\max_{\forall k,\forall m}(\beta'_{km}) \tag{12}$$

Subsequently, the private weights and other states of these coagulated particles are recalculated according to the probabilistic coagulation rule. As for the i–j coagulation event, two new simulation particles replace the "old" particles i and j, as formulated by Eq. (13):

$$\text{if } w_i \neq w_j,\begin{cases} w_i^* = \max(w_i,w_j) - \min(w_i,w_j);\ v_i^* = v_m|_{w_m=\max(w_i,w_j)};\\ \quad u_{pk,i}^* = u_{pk,m}|_{w_m=\max(w_i,w_j)};\ x_{pk,m}^* = x_{pm,k}|_{w_m=\max(w_i,w_j)}\\ w_j^* = \min(w_i,w_j);\ v_j^* = v_i + v_j;\\ \quad u_{pk,j}^* = (v_i u_{pk,i} + v_j u_{pk,j})/(v_i+v_j);\ x_{pk,j}^* = x_{pk,m}|_{w_m=\min(w_i,w_j)} \end{cases}$$

$$\text{if } w_i = w_j,\begin{cases} w_i^* = w_i/2;\ v_i^* = v_i + v_j;\\ \quad u_{pk,i}^* = (v_i u_{pk,i} + v_j u_{pk,j})/(v_i+v_j);\ x_{pk,i}^* = x_{pk,i}\\ w_j^* = w_j/2;\ v_j^* = v_i + v_j;\\ \quad u_{pk,j}^* = (v_i u_{pk,i} + v_j u_{pk,j})/(v_i+v_j);\ x_{pk,j}^* = x_{pj,k} \end{cases} \tag{13}$$

where the asterisk indicates a new value of weight or state after the coagulation event; v_i is the volume of simulation particle i; $u_{pk,i}$ and $x_{pk,i}$ are the velocity and position of particle i in the direction k. It is obvious Eq. (13) satisfies the laws of conservation of mass and momentum, and the differentially-weighted MC method is able to conserve the simulation particle number automatically.

At last, the computational cost of MC can further be reduced by the smart bookkeeping technique that is described in reference [48]. The key idea of the bookkeeping technique is to update the total coagulation rate of each simulation particle after each time interval. Since there are only a few portions of simulation particles related to coagulation events within a time interval $\Delta\tau$, the total coagulation rate of a non-coagulated simulation particle after $\Delta\tau$ can be calculated by only updating the normalized kernels between the non-coagulated simulation particles and the coagulated simulation particles (their weights and other states may change according to Eq. (13)). Double counting over all simulation particles within grid l is thus avoided during the simulation itself, and, in fact, only has to be performed at the very first time interval.

These steps are repeated until $\sum_m \Delta\tau_m \geqslant \Delta t$. In fact the last time interval is forced to $\Delta t - \sum_{m-1}\Delta\tau_m$. The flowchart of the differentially-weighted MC method for particle coagulation is presented in Fig. 3.

The differentially-weighted MC method exhibits an optimal combination of high statistical accuracy for PSD and low computational effort. For example, for a same case of Brownian coagulation (induced by Brownian motion of small particles in fluids) in the free-molecular regime (where the mean free path of gas molecules is far greater than the particle diameter), the MC method is capable of determining the particle size distribution over the full size spectrum (shown in Fig. 2), as compared to the constant-number method.

From Fig. 4 we also see MC simulation exhibits slight fluctuations for these particles smaller than $0.01\,v_{avg}$, which should be ascribed to statistical noise of MC simulation. These noise could be constrained or reduced by some ways, e.g., the shift action (used to restrict the simulation particle number of each size interval within prescribed bounds) [48], variance reduction by important sampling in MC methods [59] and rare-events simulation [60]. On the other hand, the event-driven MC simulation (where special events are implemented stochastically with probabilities derived from the mean-field rates of the corresponding process) is more accurate than the time-event MC simulation presented here because events are fully uncoupled among different time steps, on cost of more CPU time. In fact we [61] unified event-driven mode and time-driven mode of MC simulation for spatially averaged PBM. It is straightforward to couple the event-driven MC with the multiphase flow models.

3. Model validation

Depending on Stokes number (St) of particles (rather than particle size), they can be divided into three catalogues: fine particle ($St \to 0$), finite-inertia particles ($0 < St < \infty$), and coarse particles ($St \to \infty$). The analytical solutions of turbulence-induced coagulation rates were obtained only for the limiting cases such as fine zero-inertia particles [62] and coarse high-inertia [63] particles. The limiting case of coarse particles is used to validate the PBMC method for particle coagulation in a spatially inhomogeneous system. As for the coarse particles, the dynamic relaxation time is much greater than the turbulence temporal macroscale time, and particles are thus statistically independent, i.e., their relative motion is zero-correlated and is similar to the chaotic motion of molecules in kinetic theory (the so-called hypothesis of molecular chaos). This case is allowed to not take account of complex turbulent flow models and the two-ways coupling of the continuous and discrete phases, and only focus on particle motion and particle dynamics. Keep in mind that although the simulation case using for numerical validation is very special (the particles moves freely (but for coagulations) after initialization and the particle dynamics is field-independent), the numerical strategy presented here should be suitable for other real case in theory and its application in other complex cases (e.g., the flow case with shocks) is straightforward.

In the initial stage, the monodisperse particles with diameter of 0.01 (all parameters in this case are dimensionless) and with number of 10^5 are uniformly distributed in a domain $0 < x < 2\pi$,

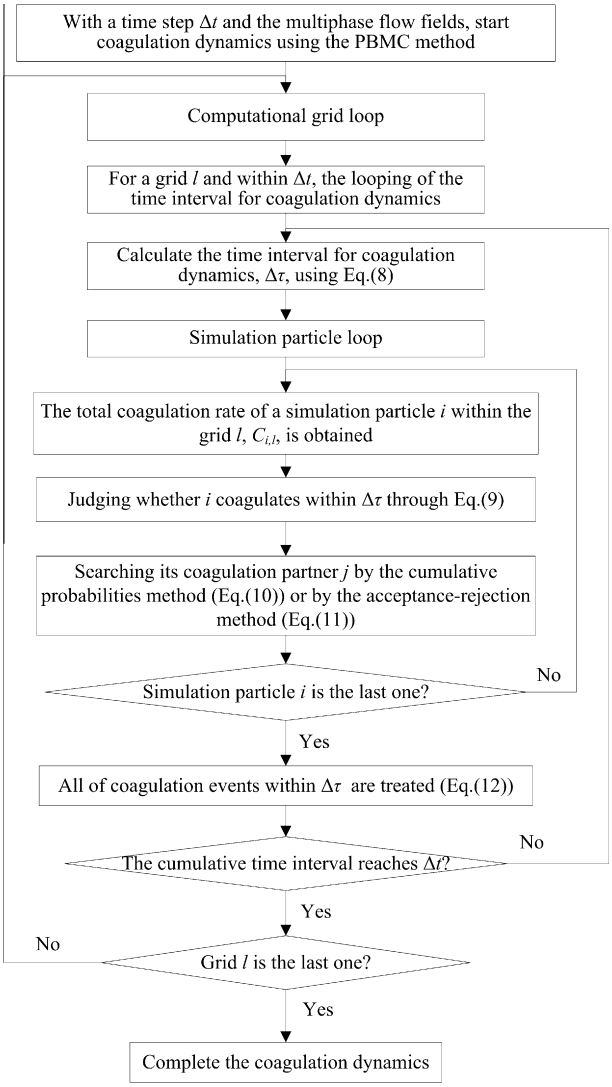

Fig. 3. The flowchart of the differentially-weighted MC method for particle coagulation.

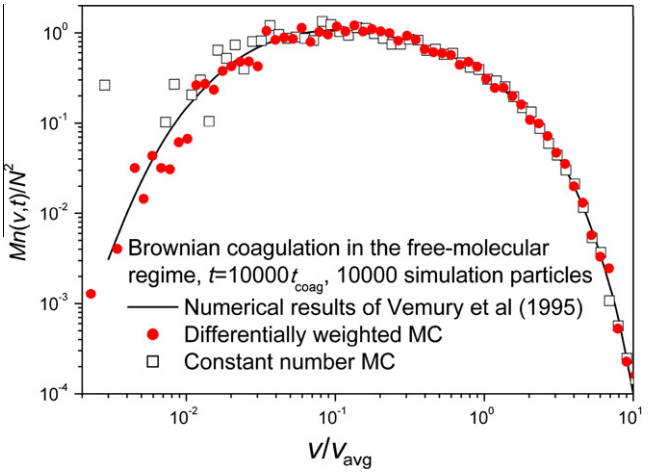

Fig. 4. Self-preserving particle size distribution for Brownian coagulation in the free-molecular regime among results obtained from the differentially-weighted MC, the constant-number method and a discrete-sectional method [58]. The dimensionless particle volume η is defined as v/v_{avg}, the dimensionless number distribution function $\Psi = Mn(v,t)/N^2$, where v_{avg} is the mean particle volume; $n(v,t)$ is the particle size distribution function at time t; M and N is the total mass concentration and number concentration of particles.

$0 < y < 2\pi$, $0 < z < 2\pi$ with periodicity applied in three directions; and the particle velocity satisfies Maxwell distribution with the average kinetic energy per unit mass ($\bar{e}_p$) of 1. Simulation particles with number of 80,000 are uniformly distributed in ($16 \times 16 \times 16$) grids, and the simulation time is set as 5.

Within the kth time-step, the position of simulation particle i is first calculated as: $(x_{pi})_k = (x_{pi})_{k-1} + (u_{pi})_{k-1}\Delta t_k$; then, if particle i does not undergo a coagulation event with the time step Δt_k, it conserves the original velocity, statistical weight and volume unaffected within Δt_k, otherwise its velocity and other states are determined by Eq. (13). In this case coagulation dynamics is controlled by the following analytical coagulation kernel [63]:

$$\beta_{ij} = [16\pi(e_{pi} + e_{pj})/3]^{1/2}(d_{pi} + d_{pj})^2/4 \quad (14)$$

where d_{pi} is the diameter of particle i, and e_{pi} is the kinetic energy per unit mass of simulation particle i. e_{pi} is calculated as $(u^2_{pi,1} + u^2_{pi,2} + u^2_{pi,3})/2$.

Although the analytical solution of coagulation kernel exists in the limiting case, it is difficult to obtain the analytical solutions of the temporal and spatial evolution of particle size distribution. Direct numerical simulation (DNS) has provided an accurate "model-free" representation of two-phase turbulent flows. The numerical result of DNS is selected as a standard reference to validate the PBMC method for particle coagulation. More details on DNS simulation are demonstrated in Refs. [64–66]. In the DNS method, every real particle is directly tracked, and the proactive method with sorting [66] is used to check for dynamic interactions between particles within a time-step.

The average collision rate per unit volume, N_c (with dimension of $m^{-3}\,s^{-1}$), is calculated in the MC and DNS methods as following:

$$N_c = N_{tc}/(\Delta t V_t) \quad (15)$$

where N_{tc} is the total number of the detected coagulation events within a time-step Δt, V_t is the volume of the computational domain. Fig. 5a demonstrates the time evolution of the average coagulation rate per unit volume predicted by the MC and DNS methods, for which analytical solution does not exist. The average coagulation rate per unit volume decreases with time due to the decreasing particle concentration along with the occurrence of coagulation event. We further calculated the relative error δ_{NC} in the average coagulation rate per unit volume. $\delta_{NC} = |N_c^{(DNS)} - N_c^{(MC)}|/N_c^{(DNS)}$, where the superscript "DNS" represents the result of the DNS simulation and "MC" means the result of the MC method. From Fig. 5b it is found the relative error δ_{NC} fluctuates within 10% and 20% on the whole. The relatively large error is ascribed to the following factors: (1) in the initialization the particles are stochastically and homogeneously distributed within the computational domain. And each particle is given stochastic velocities in three dimensions (the particle velocity satisfies Maxwell distribution with the average kinetic energy per unit mass of 1). The stochastic initialization

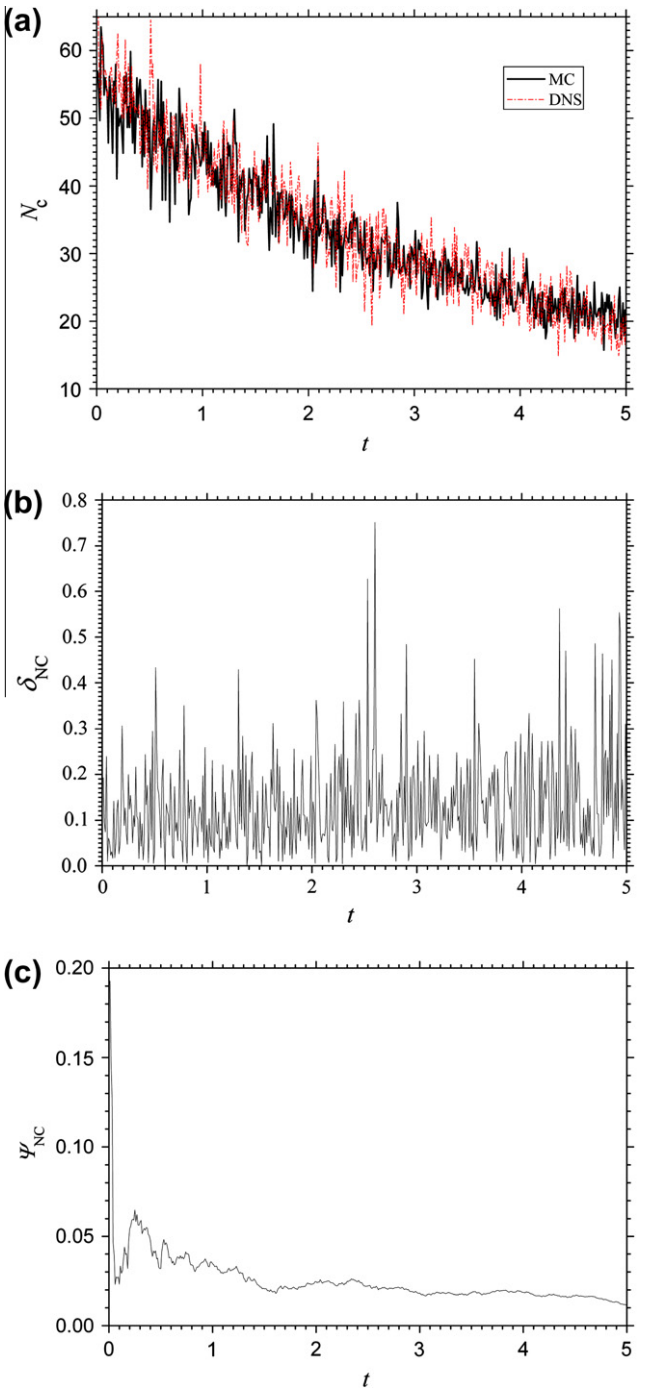

Fig. 5. The average coagulation rate per unit volume (N_c) in the coarse particles. (a) the time-evolving N_c; (b) the relative error in the average coagulation rate per unit volume (δ_{NC}); and (c) the relative error in the time-cumulative average coagulation rate per unit volume ($\psi_{NC}(t)$).

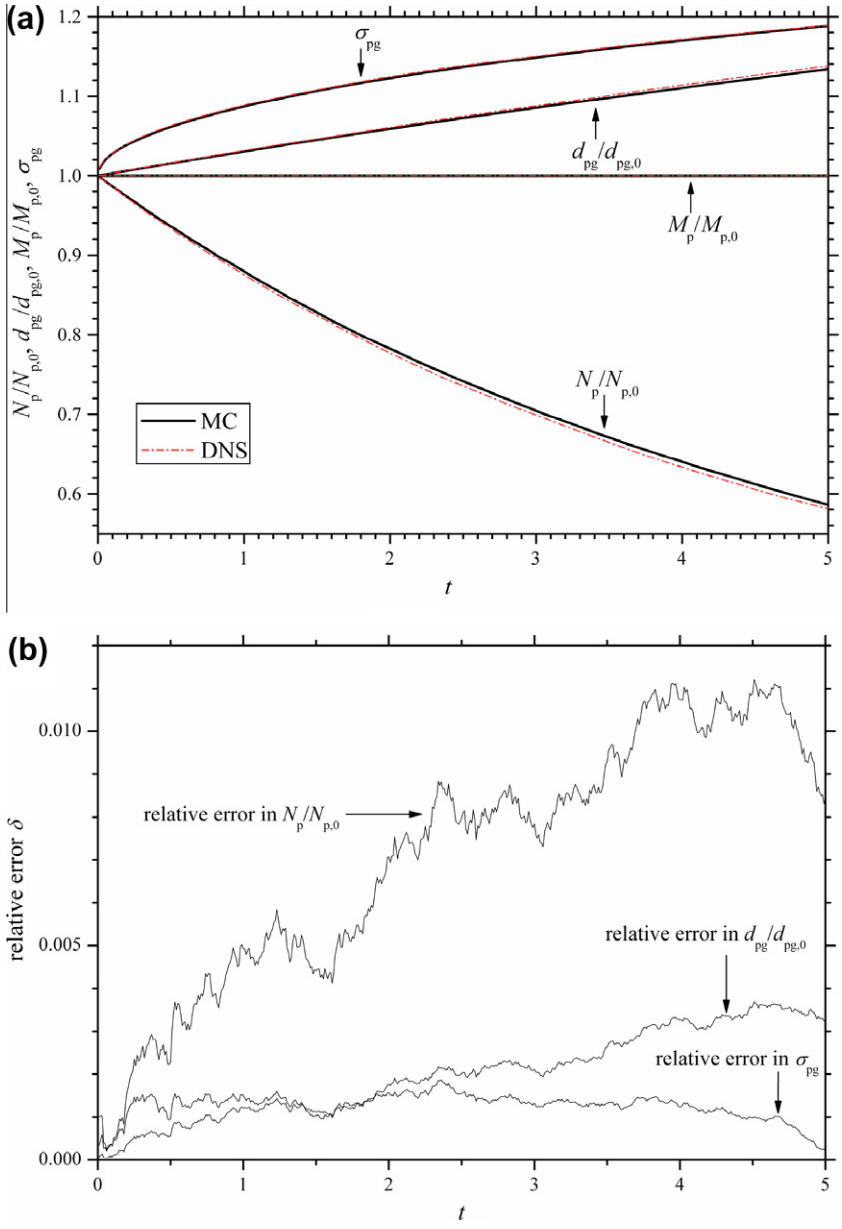

Fig. 6. (a) The time evolution of the moments of particle size distribution and (b) the relative error in the moments of particle size distribution.

makes the collision and coagulation processes between particles be stochastic to a certain extent. The coagulation rate thus fluctuates sharply as time evolves; (2) in the MC simulation the stochastic processes are utilized to determine the particle coagulation, while in the DNS simulation the coagulation events are deterministically detected based on the trajectory-crossing. Fig. 5c also shows the relative error in the time-cumulative coagulation rate, $\Psi_{NC}(t) = |\int_0^t N_c^{(DNS)}dt - \int_0^t N_c^{(MC)}dt| / \int_0^t N_c^{(DNS)}dt$. It is obvious that the time-cumulative relative error $\psi_{NC}(t)$ is generally constrained within 2% for relatively long evolution time.

Fig. 6a shows the time evolution of the moments of particle size distribution and the total particle momentum. The particle number concentration (N_p) decreases along with time, however, the geometric mean diameter (d_{pg}) increases along with time. The geometric standard deviation (σ_{pg}) deviates the initial value, 1, more and more, which indicates particle population is inclined to polydispersity along with time, or saying, the population is sized more differently. The total particle momentum (M_p) is strictly conserved in the two methods. Fig. 6b presents the relative error in the geometric mean diameter, number concentration, and geometric standard deviation. All of these relative errors are very small, generally kept below 1%. It is obvious that the results of the MC method agree well with that of DNS simulation.

The particle size distribution functions at some specified time-points are shown in Fig. 7, where the abscissa k is the number of primary particles, P_k is the probability of obtaining a aggregate containing k primary particles, or, the ratio of particles of volume v_k ($v_k = kv_0$, v_0 is the monomer volume, k is the number of primary particles) to the total particle number. The inset in the top right corner of Fig. 7, where the Y-axis (P_k) is scaled linearly instead of logarithmically (as in Fig. 7), shows the size distribution of small aggregates ($k \leqslant 5$). The MC results for these small aggregates agree well with the DNS results. With respect to these larger aggregates, although there is being a few deviations between the MC and DNS simulations, the MC method is able to reproduce qualitatively similar results as the DNS reference on the whole. Generally the MC

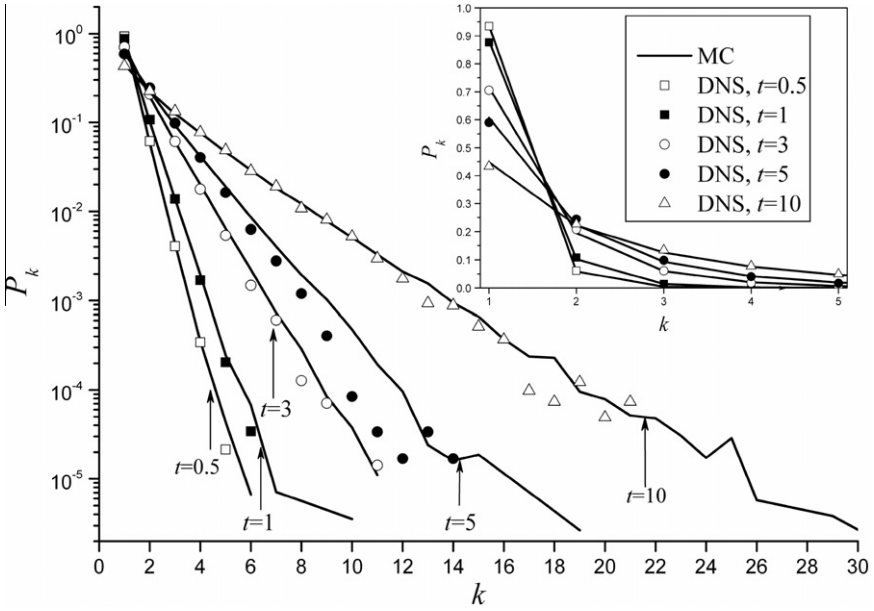

Fig. 7. Particle size distribution at the specified time points.

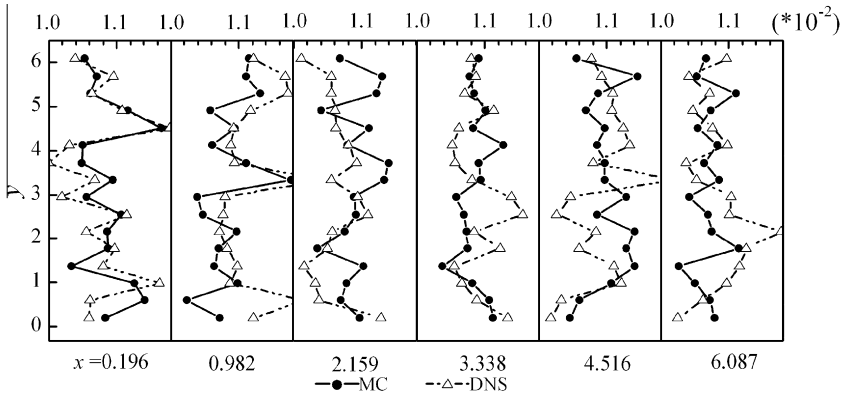

Fig. 8. The spatial distribution of geometric mean diameter of particles at the specified time point ($t = 2.5$) and section ($z = \pi$).

solution is deviating from the DNS solution as aggregates grow up. At $t = 5$ the predicted size distribution of large aggregates (with more than eight primary particles) by the MC obviously deviates from the DNS solution. In order to examine whether the numerical precision of the MC deteriorate more and more as time evolves, we further extended the evolution time (here until $t = 10$) of coagulation dynamics in the simulations. It is interesting the MC results at $t = 10$ agree better with the DNS results than at $t = 5$. It indicated that the MC does not show the trend of precision deterioration as time increases. In fact, although particle number concentration decreases and particle population is inclined to polydispersity more and more as time evolves, the new MC method is able to adapt automatically itself to the extension of particle size distribution, that is, some simulation particles with smaller private weights are reproduced automatically to represent these less-populated regions (e.g., these larger particles, $v > 8v_0$, which only occupy a few portion of number in population). Keep in mind that the PBMC is capable of tracking all particles in theory. This is highly relevant for engineering applications, since it is important that no information on the evolving particle population is lost, particularly in relation to particles that are few in number but exhibit special physical and chemical properties. The good performance of the PBMC method in noise reduction and range extension should be attributed to the differentially weighting of simulation particles, which effectively increase the number of simulation particles to represent these less-populated real particles. The results presented here provided strong support that the new MC method is capable of capturing the temporal evolution of particle size distribution with high precision.

Both the MC method and DNS can obtain the detailed information on the particle fields including the spatiotemporal distribution of particle population, the fields of particle velocity, kinetic energy, and momentum, which are determined by the ensemble averaging procedure over all simulation particles in their local grid. These temporally and spatially distributed environmental variables are further compared to one another. Fig. 8 is instantaneous geometric mean diameter (d_{pg}) at a specified time ($t = 2.5$) and at a specified two-dimensional section ($z = \pi$). The spatial distributions of particle number concentration (N_p) and particle momentum ($m_p u_p$) at the time $t = 2.5$ and the section $z = \pi$ are shown in Figs. 9 and 10, respectively. Although MC results deviate from DNS results in some regions, the two results at several specified distance in x-dimension direction, i.e., $x = 0.196$, 0.982, 2.159, 3,338, 4.516, and 6.087, evolve with similar tendency along the y-dimension direction on the whole. From these results shown in Figs. 5–10, we concluded that the new MC method is able to predict reasonably the

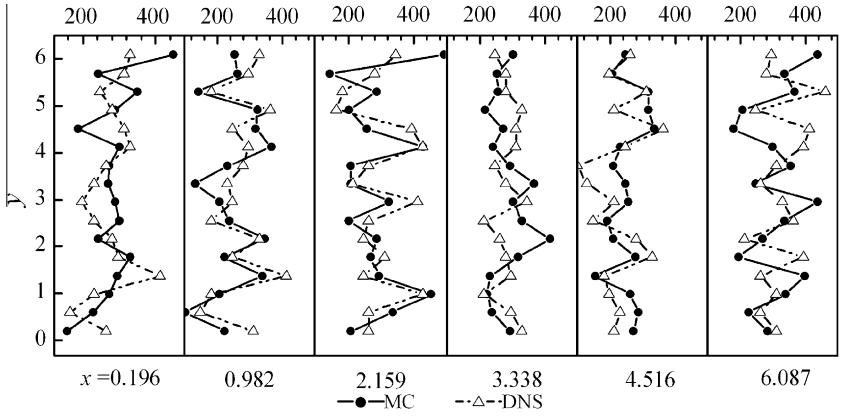

Fig. 9. The spatial distribution of number concentration of particles at the specified time point ($t = 2.5$) and section ($z = \pi$).

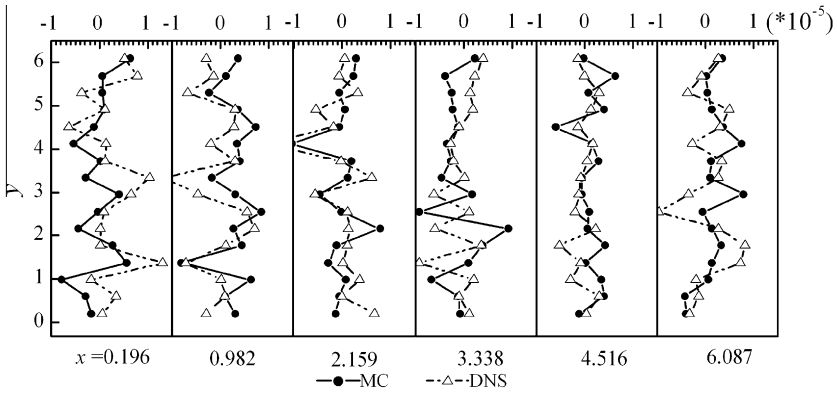

Fig. 10. The spatial distribution of momentum of particles at the specified time point ($t = 2.5$) and section ($z = \pi$).

statistical parameters such as the coagulation rate but also the temporal and spatial evolution of particle fields.

With regards to numerical difference between MC and DNS simulations in the spatial distributions of particle size distributions, we still emphasized the following two main factors (as explained for the coagulation rate): (1) the stochastic initialization for particle position and velocities, and (2) stochastic coagulation events in the MC simulation. Increasing the number of particles or the number of MC runs can make the MC results be closer to the DNS results; however, the numerical strategy for variance reduction is not very feasible in engineering application because of complex programming and extensive computational cost. The variance reduction in the spatial distribution of PSDF need be further studied in the future.

All of simulations are performed in the same desktop PC equipped with CPU of Intel(R) Core(TM)2 Quad Q9300 @2.5 GHz, memory of 3.5 GB. The computational costs of the MC and DNS are 148 s and 1460 s, respectively. The reduction of computational cost in the MC simulation owes to the less particle number and the utilization of stochastic processes to capture coagulation events. On the contrary, DNS tracks all of real particles and detects the occurrence of coagulation events based on the trajectory-crossing.

4. Conclusion and discussion

In this study, we proposed for the first time an algorithm to couple the differentially-weighted PBMC method for particle dynamics (here coagulation process) with the Eulerian–Lagrangian model for hydrodynamics. It is equivalent to solving simultaneously the population balance equation for the particulate processes and the conservation equations for the surrounding multiphase fluids. The resultant Eulerian–Lagrangian–PBMC model (or the CFD–PBM model) is able to predict the spatiotemporal evolution of particle size distribution in a spatially inhomogeneous system accounting for mutual coupling of the particle dynamics with the hydrodynamics. The coupling is based on the selection of an appropriate time-step within which the fluid transport, the particle transport and the particle dynamics are uncoupled each other and then separately and successively simulated. The evolution of systems is based on the process (the flow and particle transport, or particle dynamics) that occurs most rapidly. If particulate events such as coagulation are slow, the multiphase flow fields update due to their flow, resulting in the spatial diffusion of PSD. If on the other hand, the dynamic events of particles are fast relative to particle transport, the particle fields evolve due to their transport and dynamics, resulting in the spatiotemporal evolution of PSD.

For a limiting case of coarse high-inertia particles, the PBMC method is compared to the direct numerical simulation (DNS). It is found the PBMC method yields reasonably closer predictions of spatiotemporal PSD but its computational expense is less by a factor of 10. It is worth noting that the PBMC method is capable of guarding the statistical accuracy in determining PSD and of tracking all particles, e.g., these with low number concentrations.

Not only does the PBMC method provide a highly efficient and precise numerical scheme for the spatiotemporal evolution of PSD. It also demonstrates friendly expansibility towards the other models in different engineering and scientific fields. For example, the MC is capable of considering the elaborate collision model such as the sticking–sliding collision model and the particle–wall colli-

sions, and the other dynamic events such as breakage, condensation/evaporation, nucleation, deposition, and chemical reactions. On the other hand, the MC can be coupled to any Euler–Lagrangian models such as stochastic trajectory model and deterministic trajectory model. For example, it is possible to model the drag force through other complex models rather than a relaxation time presented in Eq. (4). The friendly expansibility is ascribed to the mutual uncoupling scheme of the flow motion, particle motion and particle dynamics.

Thanking to the good performance of the Eulerian–Lagrangian–PBMC model, it is capable of serving for the inverse problem of PBM and determining kinetic parameters of dynamic events. The inverse problem method can be utilized to determine these kernel models and model parameters (which are usually unclear for real cases but necessary for PBM) from experiments. For example, parameter identification using the inversion of the PBMC is feasible through an experimental design technique combined with a response surface methodology [67]. The inverse problem in population balance is usually based on the spatially-average PBM, and the identified model parameters cannot include the effects of spatially inhomogeneous fields and particle dynamics. The PBMC presented in the paper is able to gain the spatiotemporal evolution of PSDF and may thus explore optimal model parameters which are most close to field-dependent experimental measurements.

Although the Eulerian–Lagrangian–PBMC model (or CFD–PBM model) exhibits good performance and friendly expansibility, there is still long way for accurate control of particulate processes, optimized design and operation of corresponding process equipments. We view the CFD–PBM model presented here as a starting point to the end. One of main limitations of the CFD–PBM model for process/equipment design and control is long simulation time for large system because the Eulerian–Lagrangian model for multiphase flow fields and the PBMC for particle dynamics are both time-consuming. Considering the dramatic increase in computational power, and the emergence of new parallel computing (such as GPU parallel computing), and the improvement in CFD–PBM simulation efficiency, fast simulation to the end become more and more feasible. Other efforts for the CFD–PBM model may include capability to deal with complex and dynamic boundary conditions, ease to use for complex simulation cases, friendly interface for initialization and post-treatment, and so on.

Acknowledgements

H. Zhao was supported by "National Natural Science Foundation of China" (50876037 and 51021065), "Program for New Century Excellent Talents in University" (NECT-10-0395) and "National Key Basic Research and Development Program" (2010CB227004).

References

[1] Ramkrishna D, Mahoney AW. Population balance modeling. Promise for the future. Chem Eng Sci 2002;57(4):595–606.
[2] Gerstlauer A, Gahn C, Zhou H, Rauls M, Schreiber M. Application of population balances in the chemical industry – current status and future needs. Chem Eng Sci 2006;61(1):205–17.
[3] Kilander J, Blomström S, Rasmuson A. Spatial and temporal evolution of floc size distribution in a stirred square tank investigated using PIV and image analysis. Chem Eng Sci 2006;61(23):7651–67.
[4] Wang LP, Wexler AS, Zhou Y. Statistical mechanical description and modelling of turbulent collision of inertial particles. J Fluid Mech 2000;415:117–53.
[5] Friedlander SK. Smoke dust and haze: fundamentals of aerosol dynamics. 2nd ed. Oxford University Press; 2000.
[6] Johannessen T, Pratsinis SE, Livbjerg H. Computational fluid–particle dynamics for the flame synthesis of alumina particles. Chem Eng Sci 2000;55(1):177–91.
[7] Zucca A, Marchisio DL, Vanni M, Barresi AA. Validation of bivariate DQMOM for nanoparticle processes simulation. AIChE J 2007;53(4):918–31.
[8] Muhlenweg H, Gutsch A, Schild A, Pratsinis SE. Process simulation of gas-to-particle-synthesis via population balances: investigation of three models. Chem Eng Sci 2002;57(12):2305–22.
[9] Vikhansky A, Kraft M. Modelling of a RDC using a combined CFD-population balance approach. Chem Eng Sci 2004;59(13):2597–606.
[10] Kruis FE, Wei J, van der Zwaag T, Haep S. Computational fluid dynamics based stochastic aerosol modeling: combination of a cell-based weighted random walk method and a constant-number Monte-Carlo method for aerosol dynamics. Chem Eng Sci 2012;70:109–20.
[11] Zhao H, Kruis FE, Wei J, van der Zwaag T. Haep S, Zheng C. A spatio-temporal population balance-Monte Carlo method for diffusion and coagulation of nanoparticles in plug-flow aerosol reactors. In: European aerosol conference 2009 paper T140A04; 2009.
[12] Zhao H, Kruis FE, Wei J, Zheng C. CFD-based population balance modeling for nanoparticle convection and coagulation. In: 7th International conference on multiphase flow; 2010.
[13] Skillas G, Becker C, Muhlenweg H, Behnisch J. Simulation of particulates in a carbon black reactor. J Nanopart Res 2005;7(1):15–27.
[14] Settumba N, Garrick SC. A comparison of diffusive transport in a moment method for nanoparticle coagulation. J Aerosol Sci 2004;35(1):93–101.
[15] Kalani A, Christofides PD. Nonlinear control of spatially inhomogenous aerosol processes. Chem Eng Sci 1999;54(13–14):2669–78.
[16] Kalani A, Christofides PD. Simulation, estimation and control of size distribution in aerosol processes with simultaneous reaction, nucleation, condensation and coagulation. Comput Chem Eng 2002;26(7–8):1153–69.
[17] Kazakov A, Frenklach M. Dynamic modeling of soot particle coagulation and aggregation: implementation with the method of moments and application to high-pressure laminar premixed flames. Combust Flame 1998;114(3–4):484–501.
[18] Balthasar M, Mauss F, Knobel A, Kraft M. Detailed modeling of soot formation in a partially stirred plug flow reactor. Combust Flame 2002;128(4):395–409.
[19] Balthasar M, Mauss F, Wang H. A computational study of the thermal ionization of soot particles and its effect on their growth in laminar premixed flames. Combust Flame 2002;129(1–2):204–16.
[20] Balthasar M, Frenklach M. Detailed kinetic modeling of soot aggregate formation in laminar premixed flames. Combust Flame 2005;140(1–2):130–45.
[21] Falk L, Schaer E. A PDF modelling of precipitation reactors. Chem Eng Sci 2001;56(7):2445–57.
[22] Wilck M, Stratmann F. A 2-D multicomponent modal aerosol model and its application to laminar flow reactors. J Aerosol Sci 1997;28(6):959–72.
[23] Zucca A, Marchisio DL, Barresi AA, Fox RO. Implementation of the population balance equation in CFD codes for modelling soot formation in turbulent flames. Chem Eng Sci 2006;61(1):87–95.
[24] Jeong JI, Choi M. Analysis of non-spherical polydisperse particle growth in a two-dimensional tubular reactor. J Aerosol Sci 2003;34(6):713–32.
[25] Lockwood FC, Yousif S. A model for the particulate matter enrichment with toxic metals in solid fuel flames. Fuel Process Technol 2000;65–66(1):439–57.
[26] Kim D, Gautam M, Gera D. Parametric studies on the formation of diesel particulate matter via nucleation and coagulation modes. J Aerosol Sci 2002;33(12):1609–21.
[27] Kim DH, Gautam M, Gera D. Modeling nucleation and coagulation modes in the formation of particulate matter inside a turbulent exhaust plume of a diesel engine. J Colloid Interface Sci 2002;249(1):96–103.
[28] Wen JZ, Thomson MJ, Park SH, Rogak SN, Lightstone MF. Study of soot growth in a plug flow reactor using a moving sectional model. Proc Combust Inst 2005;30(1):1477–84.
[29] Nere NK, Ramkrishna D. Solution of population balance equation with pure aggregation in a fully developed turbulent pipe flow. Chem Eng Sci 2006;61(1):96–103.
[30] Pyykönen J, Jokiniemi J. Computational fluid dynamics based sectional aerosol modelling schemes. J Aerosol Sci 2000;31(5):531–50.
[31] Hollander ED, Derksen JJ, Bruinsma OSL, van den Akker HEA, van Rosmalen GM. A numerical study on the coupling of hydrodynamics and orthokinetic agglomeration. Chem Eng Sci 2001;56(7):2531–41.
[32] Balthasar M, Kraft M. A stochastic approach to calculate the particle size distribution function of soot particles in laminar premixed flames. Combust Flame 2003;133(3):289–98.
[33] Singh J, Balthasar M, Kraft M, Wagner W. Stochastic modeling of soot particle size and age distributions in laminar premixed flames. Proc Combust Inst 2005;30(1):1457–65.
[34] Zhao B, Yang ZW, Johnston MV, Wang H, Wexlerd AS, Balthasard M, et al. Measurement and numerical simulation of soot particle size distribution functions in a laminar premixed ethylene oxygen–argon flame. Combust Flame 2003;133(1–2):173–88.
[35] Kolodko A, Sabelfeld K, Wagner W. A stochastic method for solving Smoluchowski's coagulation equation. Math Comput Simulat 1999;49(1–2):57–79.
[36] Sabelfeld K, Kolodko A. Stochastic Lagrangian models and algorithms for spatially inhomogeneous Smoluchowski equation. Math Comput Simulat 2003;61(2):115–37.
[37] Kruis FE, Wei J, van der Zwaag T, Haep S. Computational fluid dynamics based stochastic aerosol modeling: combination of a cell-based weighted random walk method and a constant-number method for aerosol dynamics. In: 4th International conference on population balance modelling; 2010.
[38] Qamar S, Ashfaq A, Warnecke G, Angelov I, Elsner MP, Seidel-Morgenstern A. Adaptive high-resolution schemes for multidimensional population balances in crystallization processes. Comput Chem Eng 2007;31(10):1296–311.

[39] Garrick SC, Lehtinen KEJ, Zachariah MR. Nanoparticle coagulation via a Navier–Stokes/nodal methodology: evolution of the particle field. J Aerosol Sci 2006;37(5):555–76.
[40] Dorao CA, Jakobsen HA. Application of the least-squares method for solving population balance problems in R^{d+1}. Chem Eng Sci 2006;61:5070–81.
[41] Dorao CA, Jakobsen HA. Time–space-property least squares spectral method for population balance problems. Chem Eng Sci 2007;62(5):1323–33.
[42] Campos FB, Lage PLC. A numerical method for solving the transient multidimensional population balance equation using an Euler–Lagrange formulation. Chem Eng Sci 2003;58(12):2725–44.
[43] Lu SY, Lin HC, Lin CH. Modeling particle growth and deposition in a tubular CVD reactor. J Cryst Growth 1999;200(3–4):527–42.
[44] Brown DP, Kauppinen EI, Jokiniemi JK, Rubin SG, Biswas P. A method of moments based CFD model for polydisperse aerosol flows with strong interphase mass and heat transfer. Comput Fluids 2006;35(7):762–80.
[45] Yeoh GH, Tu JY. Two-fluid and population balance models for subcooled boiling flow. Appl Math Model 2006;30(11):1370–91.
[46] Smith M, Matsoukas T. Constant-number Monte Carlo simulation of population balances. Chem Eng Sci 1998;53(9):1777–86.
[47] Lin Y, Lee K, Matsoukas T. Solution of the population balance equation using constant-number Monte Carlo. Chem Eng Sci 2002;57(12):2241–52.
[48] Zhao H, Kruis FE, Zheng C. Reducing statistical noise and extending the size spectrum by applying weighted simulation particles in Monte Carlo simulation of coagulation. Aerosol Sci Tech 2009;43(8):781–93.
[49] Zhao H, Zheng C. A new event-driven constant-volume method for solution of the time evolution of particle size distribution. J Comput Phys 2009;228(5):1412–28.
[50] Patterson RIA, Wagner W, Kraft M. Stochastic weighted particle methods for population balance equations. J Comput Phys 2011;230(19):7456–72.
[51] DeVille REL, Riemer N, West M. Weighted flow algorithms (WFA) for stochastic particle coagulation. J Comput Phys 2011;230(23):8427–51.
[52] Zhou L. Theory and numerical modeling of turbulent gas-particle flows and combustion. CRC Press; 1993.
[53] Sommerfeld M. Validation of a stochastic Lagrangian modelling approach for inter-particle collisions in homogeneous isotropic turbulence. Int J Multiphas Flow 2001;27(10):1829–58.
[54] Bird GA. Molecular gas dynamics and the direct simulation of gas flow. Oxford Science Publ.; 1994.
[55] Crowe CT, Sharma MP, Stock DE. The particle source in cell (PSI-CELL) model for gas droplet flows. J Fluid Eng – Trans ASME 1977;99(2):325–31.
[56] Gosman AD, Ionnides IE. Aspects of computer simulation of liquid fuelled combustors. AIAA paper 81-0323; 1981.
[57] Mehrotra V, Silcox GD, Smith PJ. Numerical simulation of turbulent particle dispersion using a Monte Carlo approach. ASME fluids engineering division summer meeting paper FEDSM98-5036; 1998.
[58] Vemury S, Pratsinis SE. Self-preserving size distributions of agglomerates. J Aerosol Sci 1995;26(2):175–85.
[59] Srinivasan R. Importance sampling – applications in communications and detection. Springer-Verlag; 2002.
[60] Bucklew JA. Introduction to rare event simulation. Springer- Verlag; 2004.
[61] Zhao H, Kruis FE, Zheng C. A differentially weighted Monte Carlo method for two-component coagulation. J Comput Phys 2010;229(19):6931–45.
[62] Saffman PG, Turner JS. On the collision of drops in turbulent clouds. J Fluid Mech 1956;1:16–30.
[63] Abrahamson J. Collision rates of small particles in a vigorously turbulent fluid. Chem Eng Sci 1975;30(11):1371–9.
[64] Wang LP, Wexler AS, Zhou Y. On the collision rate of small particles in isotropic turbulence. I. Zero-inertia case. Phys Fluids 1998;10(1):266–76.
[65] Reade WC, Collins LR. A numerical study of the particle size distribution of an aerosol undergoing turbulent coagulation. J Fluid Mech 2000;415:45–64.
[66] Sundaram S, Collins LR. Numerical considerations in simulating a turbulent suspension of finite-volume particles. J Comput Phys 1996;124(2):337–50.
[67] Braumann A, Kraft M, Mort PR. Parameter estimation in a multidimensional granulation model. Powder Technol 2010;197(3):196–210.